Journal of Environmental Chemical Engineering 14 (2026) 122922

Contents lists available at ScienceDirect

Journal of Environmental Chemical Engineering

journal homepage: www.elsevier.com/locate/jece

Facile green transformation of alkali lignin via laccase-mediated functionalization for high-performance lignin-based films

Jieyu Yang [a], Yingjie Wang [a], Yu Qin [a], Mizi Fan [b,*], Guanben Du [a,*], Yan Xia [a,*], Xiaojian Zhou [a], Yonghui Zhou [c], Jingjing Liao [d]

[a] Yunnan Provincial Key Laboratory of Wood and Bamboo Biomass Materials, Southwest Forestry University, Kunming 650224, China
[b] College of Engineering, Design and Physical Sciences, Brunel University London, Uxbridge UB8 3PH, UK
[c] College of Materials and Energy, South China Agricultural University, Guangzhou 510642, China
[d] College of Landscape and Horticulture, Yunnan Agricultural University, Kunming 650201, China

ARTICLE INFO

Keywords:
Lignin
Enzymatic activation
Lignin-based film
Biocatalysis
Structure-property

ABSTRACT

Valorising alkali lignin (AL), a biorenewable pulping byproduct, is essential for advancing a circular bio-economy. However, its inherent low reactivity limits its potential as a petroleum-polyol substitute. This study developed a green biocatalytic strategy using *Trametes versicolor*-derived laccase to activate AL efficiently under mild, environmentally benign conditions. The results demonstrated that this enzymatic modification approach effectively increased the hydroxyl content and chemical accessibility of lignin, facilitating its transformation from a low-value filler into a functional co-polyol. The analysis results also confirmed that the elevated concentration of reactive -OH groups significantly enhanced both the homogeneity and the crosslinking density within the lignin-polyurethane network by reducing steric hindrance. When lignin content reached 30%, the laccase-modified lignin-based films (LMLPFs) exhibited a higher performance in both tensile strength and elasticity modulus compared to unmodified lignin-based films (LPFs), reaching values of 31.49 MPa (increased 25%) and 215.23 MPa (increased 60%), respectively, compared to 25.21 MPa and 134.40 MPa for LPFs. Furthermore, the thermal stability of LMLPFs was also improved, with the decomposition temperature at 5% mass loss ($T_{5\%}$) increasing from 277 ℃ (LPFs) to 280 ℃. By replacing fossil-derived components with enzymatically valorised biopolymers through an energy-efficient process, this work provides a feasible, sustainable pathway for the design of advanced lignin-based biocomposites.

1. Introduction

Lignin, one of the most abundant biorenewable materials and a by-product of the papermaking and biorefinery industries, amounts to 50–70 million tons per year [1,2]. Due to its phenyl structure and diverse functional groups, lignin has emerged as a promising aromatic precursor with extensive applicability [3–5]. Recently, lignin has been successfully engineered into multifunctional degradable nanocomposite fibres for UV-shielding, antimicrobial, and radioactive iodine trapping applications [6], and has further demonstrated considerable potential as high-performance supercapacitor materials [7,8]. These lignin-derived sustainable materials not only mitigate environmental impacts but also exhibit broad application prospects. In particular, lignin has been widely utilised in the development of composite membranes, exemplified by its incorporation into polyurethanes [9,10]. However, the utilisation of lignin is significantly limited by its low chemical reactivity, stemming from the complex, heterogeneous, and highly branched architecture that renders many of its hydroxyl groups, particularly phenolic hydroxyls, poorly accessible due to steric hindrance, while also leading to poor solubility and dispersibility within the polyurethane reaction medium, thereby impeding the formation of a homogeneous polymer network [11]. Consequently, the direct utilisation of unmodified lignin as a polyol precursor typically presents fundamental technical obstacles such as high brittleness and poor mechanical properties, which severely restricts their practical applications [12].

Strategic modification of lignin is essential to enhance its suitability as a polyol substitute. Conventional chemical modification processes can address these limitations, but they often require high temperature and pressure and generate environmental pollutants, thus suffer from harsh conditions, volatile organic solvents and high costs [13–16]. In

* Corresponding authors.
E-mail addresses: Mizi.Fan@brunel.ac.uk (M. Fan), gongben9@hotmail.com (G. Du), xiayanswfu@gmail.com (Y. Xia).

https://doi.org/10.1016/j.jece.2026.122922
Received 13 February 2026; Received in revised form 8 April 2026; Accepted 28 April 2026
Available online 30 April 2026

contrast, enzymatic approaches offer a greener alternative. This biocatalytic approach aligns with the principles of green chemistry, offering distinct advantages such as mild reaction conditions, minimal environmental impact, and the generation of water as the sole by-product [17]. Enzymatic modification presents a compelling alternative, yet most previous studies employed purified or commercial laccase, which, although ensuring well-defined activity, inevitably increased processing cost and complexity [18,19]. In nature, white-rot fungi are well-known for their potent ability to modify lignin, which is attributed to the secretion of extracellular enzymes such as lignin peroxidases (LiPs), manganese peroxidases (MnPs), and laccases [20,21].

HBT and other mediators have been used to enhance laccase activity toward lignin, but the direct use of unpurified fungal culture broth in combination with a laccase-mediator system has rarely been explored as a low-cost alternative. While laccase-modified lignin and lignin-based polyurethane have been independently reported, an integrated study encompassing enzymatic activation, structural characterisation, and systematic evaluation of the resulting polyurethane film properties within a single framework remains lacking. To address these limitations, the crude laccase (directly secreted from white rot fungus, without purification) /HBT-mediated modification developed in this work achieves simultaneous enhancement of both aliphatic and phenolic hydroxyl content under mild aqueous conditions, resulting in PU films with superior comprehensive performance. This strategy offers a low-cost, energy-efficient, and environmentally friendly route for preparing high-performance lignin-based PU films.

This work develops a cost-effective and environmentally benign process in which crude *T. versicolor* broth, obtained through targeted induction of a laccase-predominant lignin oxidative enzyme system, is directly employed with HBT as a mediator to modify lignin under mild conditions. The central hypothesis is that the introduction of HBT substantially enhances the enzymatic oxidation capacity of this crude laccase system, enabling effective depolymerisation of lignin, reducing steric hindrance, and increasing the number of accessible hydroxyl groups, thereby yielding laccase-modified lignin (LML) with enhanced reactivity and compatibility. This enables LML to function as a more effective crosslinker and reinforcing agent within the polyurethane matrix, ultimately producing bio-based polyurethane films (LMLPFs) with substantially improved thermal stability and mechanical performance. This approach provides a promising route for transforming low-cost, waste lignin into high-performance, bio-based functional materials, simultaneously achieving high-value utilisation of lignin and reducing environmental pollution.

2. Materials and methods

2.1. Materials

The white-rot fungus used in this study was *Trametes versicolor* (L.) Lloyd (*T. versicolor*), obtained from the China Forestry Culture Collection Centre (CFCC). Alkali lignin (AL) (97%) was supplied by Shandong Longli Co. Ltd. 1,6-Diisocyanatohexane (HDI, 99%) and Polyethylene glycol (PEG 300) were of analytical grade and supplied by Shanghai Macklin Biochemical Co., Ltd. N, N-Dimethylformamide (DMF, 99.5%) and 1,4-Dioxane (99.5%) were supplied by Guangdong Guanghua Sci-Tech Co. Ltd.

2.2. Modification of lignin and preparation of lignin-based films

2.2.1. Modification of lignin

T. versicolor. was cultivated in potato dextrose broth (PDB) supplemented with a trace element solution ($KHPO_4$, $MgSO_4{\cdot}7\ H_2O$, $CuSO_4{\cdot}5\ H_2O$, $FeSO_4{\cdot}7\ H_2O$) at 28 ℃ under shaking conditions (180 rpm) for 5 days. On day 5, the culture broth was collected and centrifuged to remove mycelia and cell debris. The resulting cell-free supernatant was used as the crude laccase preparation. Laccase activity of crude supernatant was determined then diluted with sodium acetate buffer (0.1 mol/L, pH 4.5) to a standardised activity of 200 U/L.

For the enzymatic modification reaction, 1 g of AL and 0.5 μmol of the mediator 1-hydroxybenzotriazole (HBT) were added to 100 mL of the laccase solution (200 U/L, pH 4.5). The mixture was incubated for 1 h at 40 ℃ in an orbital shaker (180 rpm). The reaction was quenched in an ice bath, and the resulting LML was recovered, washed with distilled water, and dried to constant weight at 50 ℃.

2.2.2. Assessments of the laccase-driven ligninolytic enzyme system

All spectrophotometric assays were performed in cuvettes with a 1 cm optical path length. Laccase activity was assayed at 420 nm by monitoring the oxidation of 2,2'-azinobis (3-ethylbenzthiazoline-6-sulfonate) (ABTS). LiP and MnP enzyme activities were measured via H_2O_2-dependent oxidation of veratryl alcohol (310 nm) and Mn (II) (240 nm) respectively, according to previously established methods [22]. One unit (U) was defined as the amount of enzyme producing 1 μmol of product per minute. Enzyme activity measurements were performed in triplicate. The reproducibility and precision of the assays were assessed using the coefficient of variation.

2.2.3. Preparation of lignin-based films

Lignin-based films were fabricated by reacting lignin with HDI. The polyol components consisted of lignin (AL or LML) and polyethylene glycol (PEG), where lignin was incorporated at 10%, 20%, and 30% by weight of the total polyol components [23]. The polyol components were dissolved in DMF (10 mL) and 1, 4-dioxane (5 mL). HDI was then added dropwise to the mixture to achieve an NCO/OH molar ratio of 1.1, leading to the formation of a prepolymer under continuous stirring at room temperature for 60 min. The resulting prepolymer was then cast into a mold, pre-cured at room temperature for 2 h, and cured at 80 ℃ for 8 h.

2.3. Structural characterisation for modified lignin

2.3.1. FTIR spectroscopy

FTIR spectra were recorded on a Model 650 spectrometer. Powder samples (AL and LML) were prepared with KBr pellets (1:100, w/w) and scanned in transmission mode from 4000 to 500 cm^{-1} wavenumber range at a resolution of 4 cm^{-1} over 32 scans. Lignin-based films were analysed using an attenuated total reflectance (ATR) accessory under the same wavenumber range, with a resolution of 2 cm^{-1}.

2.3.2. NMR analysis

NMR spectroscopy was employed to characterise the lignin structure. For 2D-HSQC NMR, 10 mg dried lignin specimens were dissolved in 0.5 mL DMSO-d6 (99.5%), and the resulting spectra were analysed using TopSpin software. For quantitative ^{31}P NMR analysis, dried lignin (20 mg) was dissolved in 0.5 mL of $CDCl_3$ and anhydrous pyridine (1.6:1, v/v). Subsequently, 100 μL of cyclohexanol internal standard (IS) and 0.1 mL relaxation agent solution (5 mg/mL) were added. Phosphitylation was performed by adding 100 μL of TMDP (2-chloro-4,4,5,5-tetramethyl-1,3,2-dioxaphospholane). The mixture was vortexed thoroughly to ensure complete reaction before analysis.

2.3.3. Gel permeation chromatography analysis

Lignin samples were acetylated with an acetic anhydride/pyridine mixture (1:1, v/v) at room temperature for 48 h prior to analysis. The acetylated samples were dissolved in HPLC-grade tetrahydrofuran (THF) at a concentration of 2 mg/mL and filtered through 0.22 μm polytetrafluoroethylene (PTFE) syringe filters. Molecular weight distribution was determined using a GPC system equipped with a refractive index (RI) detector, with THF as the eluent at a flow rate of 1.0 mL/min and a column temperature of 30 ℃.

2.3.4. X-ray photoelectron spectroscopy

The surface elemental composition and chemical states of the lignin samples were analysed using an X-ray photoelectron spectrometer (Thermo Scientific K-Alpha). Survey scans were performed to identify the overall elemental composition. For sample preparation, the lignin powder was uniformly pressed onto clean indium foil and subsequently dried in a vacuum oven at room temperature for 24 h prior to measurement.

2.4. Assessments of lignin-based films

2.4.1. Morphological homogeneity and interfacial compatibility

The samples were frozen in liquid nitrogen for 5 min and subsequently cryo-fractured. The fractured samples were vertically mounted on SEM stubs using conductive carbon tape and sputter-coated with gold for 90 s under vacuum. The cross-sectional morphologies of the samples were observed using a field-emission scanning electron microscope (ZEISS Sigma 300), and images were acquired in the secondary electron (SE) detector mode. The pore size of the films was quantified from SEM micrographs using ImageJ software. The pore boundaries were manually identified and measured using the "Analyse Particles" function in ImageJ.

2.4.2. Network density and swelling behaviour

The crosslink density (υ_c/V_0) of films was determined via equilibrium swelling experiments. Dried film samples (ca 0.2–0.25 g) were weighed and immersed in 20 mL DMF at 25 ℃ [24]. Subsequently, the swollen film samples were removed from the solvent, using absorbent tissue to remove excess DMF on the sample surface, and then weighed. The samples were repeated five times to check the reproducibility of the data. The crosslink density was calculated using Eq. (1) [24]. In this equation, υ_c is the effective number of crosslink chains, V_0 is the dry polymer film volume, V_1 is the DMF molar volume (76.87 mL/mol), χ is PU–DMF interaction parameter (0.40), υ is the volume fraction of PU in the total swollen film ($\upsilon = V_0/V$), where V is the volume at equilibrium of swollen mass (cm^3) [24].

$$\frac{\upsilon_c}{V_0} = \frac{-2[\upsilon + \chi v^2 + \ln(1+v)]}{V_1(2v^{1/3} - v)} \quad (2)$$

The swelling percentage (S%) was calculated using Eq. (2) [25]. In this equation, W is the weight of the films at 7 day, W_0 is the weight of the films at 0 day. Besides, the film's crystallinity degree was evaluated from the X-ray diffractograms obtained using an X-ray diffractometer (Rigaku Miniflex 600, Japan). Measurements were made in the 2θ range from 5 to 60 with a 10-degree per minute. The crystallinity index (CrI) was determined using the peak area method. The raw XRD data were first processed using MDI Jade software to perform baseline correction and peak deconvolution. The CrI value was then obtained by calculating the ratio of the total crystalline peak area to the sum of the crystalline and amorphous peak areas.

$$S\% = \left(\frac{W - W_0}{W_0}\right) \times 100\% \quad (2)$$

2.4.3. Mechanical performance

The tensile properties of the polyurethane films were evaluated using an automatic tensile tester. Rectangular specimens with dimensions of 70 mm × 10 mm × 1.3 mm (length × width × thickness) were prepared according to the Chinese National Standard GB 1302–91. Tensile tests were performed at room temperature with a crosshead speed of 25 mm/min. For each film formulation, a sample was tested five times, and the results are reported as the average value ± standard deviation.

2.4.4. Thermal stability

Thermal stability was evaluated using thermogravimetric analysis (TGA, TA Instruments Q5000). Before analysis, the samples (5–10 mg) were dried overnight at 105 °C. The analysis was performed under a nitrogen atmosphere (20 mL/min), with the samples heated from 35 ℃ to 700 ℃ at a heating rate of 10 ℃/min. Glass transition temperatures (T_g) were determined using a TA Instruments Discovery DSC 250. Samples (10–20 mg) were sealed in aluminum crucibles and analysed under nitrogen (20 mL/min). To erase thermal history, the samples underwent a heat-cool-heat cycle: they were initially heated to 80 °C and held isothermally for 3 min, then cooled to −80 ℃, and finally reheated to 200 ℃. The T_g was determined from the second heating scan, with all ramps conducted at a rate of 20 ℃/min.

2.4.5. Dynamic mechanical analysis

The dynamic mechanical properties of the lignin-based films were characterised using a dynamic mechanical analyser (DMA Q800, TA Instruments). The films were cut into rectangular specimens with dimensions of approximately 20 mm × 5 mm × 2 mm (length × width × thickness). Measurements were conducted in tensile mode under a nitrogen atmosphere at a frequency of 1 Hz, with a heating rate of 10 ℃/min over a temperature range from −50 ℃ to 150 ℃.

2.5. Statistical analysis

All quantitative experiment results were expressed as mean ± standard deviation. Statistical analysis was performed using ANOVA followed by Tukey's post-hoc test with SPSS software. Differences were considered statistically significant at $p < 0.05$.

3. Results and discussion

3.1. Structural evolution and reactivity enhancement of lignin

The detailed structural changes in lignin resulting from laccase modification were elucidated by HSQC NMR analysis, as presented in Fig. 1A. The spectra revealed distinct variations between the control and LML samples, particularly within the aliphatic region, with the former exhibiting clear and intense characteristic peaks corresponding to substructures including β-O-4 alkylaryl ethers (A), β-β resinols (B), and β-5 phenylcoumarans (C), whereas these signals were substantially diminished for the latter. It can be clearly observed that Aα, Aβ (S), Aβ (G), Aγ, Bα, Bγ, Cα, Cβ and Cγ were notably more vulnerable to cleavage, demonstrating significant laccase-mediated cleavage of β-O-4 aryl ether bonds and partial depolymerisation resulting in oligomeric fragments with M_w of approximately 377 g/mol. Conversely, the aromatic region of the LML spectrum showed no significant signal degradation, suggesting minimal cleavage of the aromatic lignin structure during laccase modification and effective preservation of the benzene ring framework. In addition, the signals corresponding to the methoxy groups (OMe) and Aγ decreased, revealing that demethoxylation occurred during laccase modification of lignin, which produced more OH groups and the number of functional groups available for chemical reactions, and thereby enhanced the reactivity of lignin [26,27].

Fig. 1B and Fig. 1C quantitatively analysed the hydroxyl groups of AL and LML using ^{31}P NMR spectroscopy, and proved that the aliphatic hydroxyl content in LML (1.52 mmol/g) was significantly higher than that in AL (1.21 mmol/g). This increase in lignin hydroxyl value resulted in a higher concentration of reactive -OH groups since the aliphatic -OH groups are the key to the reaction with isocyanate. Mechanistically, laccase-mediated demethoxylation and β-O-4 cleavage effectively exposed a higher density of reactive hydroxyl sites, reducing the steric constraints of lignin. This structural activation transformed lignin from a passive filler into an active crosslinker, significantly promoting urethane bond (-NH-COO-) formation. Consequently, this led to a much denser and more robust three-dimensional crosslinking network, directly laying the structural foundation for the enhanced mechanical strength and thermal stability observed in the LMLPFs.

As shown in Table 1, both the molecular weight and polydispersity

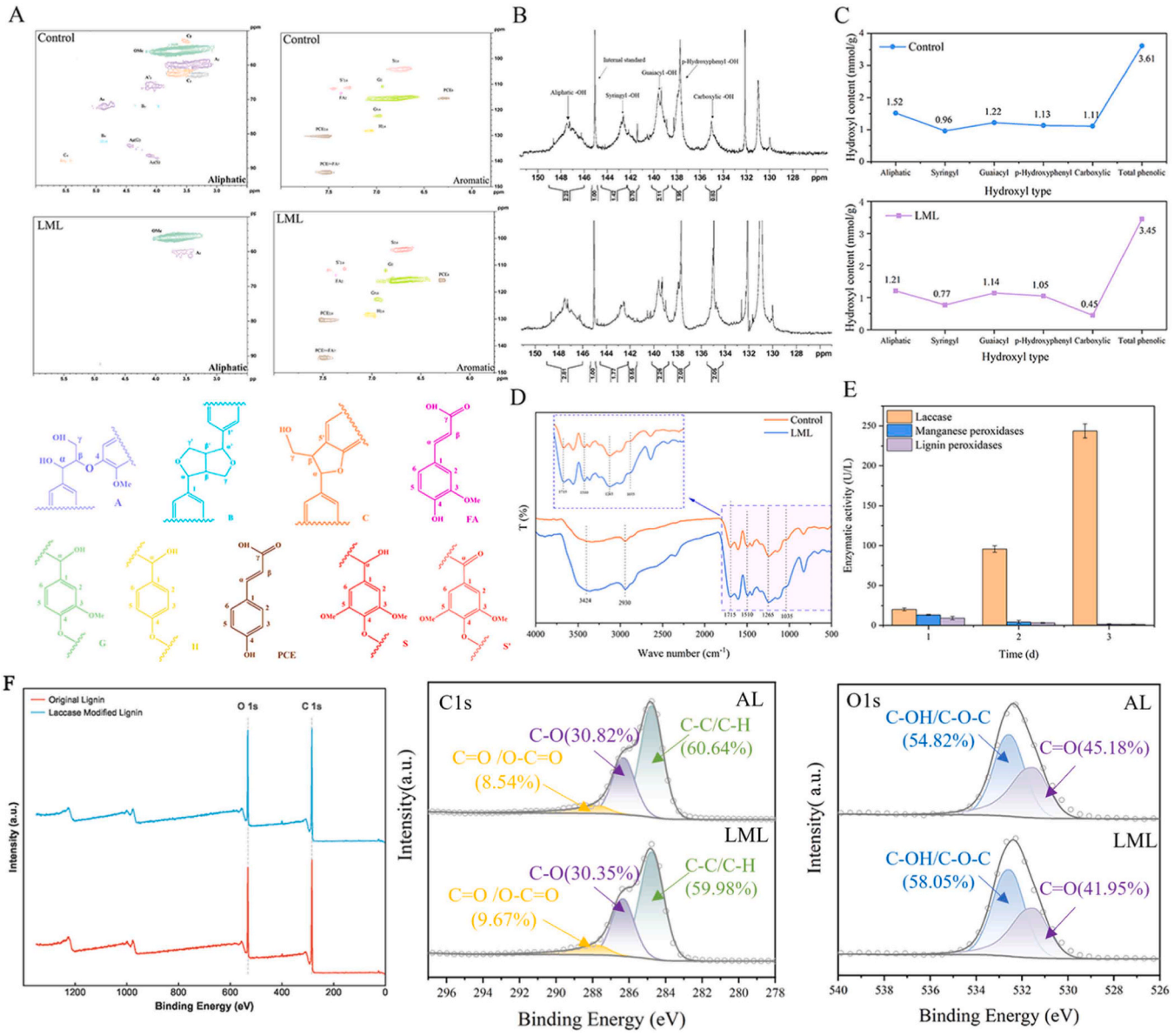

Fig. 1. Structural evolution and reactivity enhancement of lignin: A. 2D-HSQC NMR spectra of control and LML and the main identified substructures of the lignin, B. ^{31}P NMR spectra of control (top) and LML (bottom), C. hydroxyl content of control and LML, D. FTIR spectrum of lignin and LML, E. enzymatic activities of ligninolytic enzymes. F. XPS analysis of lignin: survey spectra (left), high-resolution C 1 s (middle) and O 1 s (right) spectra of AL and LML.

Table 1
Molecular weight determination results of control and LML.

	M_n/g.mol^{-1}	M_w/g.mol^{-1}	PDI
AL	408	3673	9.00245
LML	221	377	1.705882

index (PDI) of laccase-modified lignin were lower than those of unmodified lignin, indicating that depolymerisation was the dominant reaction under the conditions employed. Laccase primarily cleaves the β-O-4 linkages in lignin, depolymerisation of lignin macromolecules to micromolecules, which leads to a decrease in both M_w and M_n. When a mediator is introduced, the oxidised mediator can further access polymeric units with higher redox potentials, resulting in a greater extent of depolymerisation. Meanwhile, the decrease in PDI indicates a narrower molecular weight distribution after modification. This is because segments with high molecular weights or loose structures are degraded, reducing the proportion of large fractions in the system. A more uniform lignin feedstock contributes to a homogeneous crosslinked network in the subsequent polyurethane preparation and reduces the likelihood of defects such as localised unreacted regions or stress concentrations caused by macromolecular aggregation.

FTIR analysis further confirmed the effect of laccase modification of lignin functional groups (Fig. 1D). The intensified broad band at 3424 cm^{-1} confirmed the substantial increase in the hydroxyl group content [28], which was supported by the attenuation of peak 1265 cm^{-1}, providing complementary evidence for the cleavage of β-O-4 bonds and contributing to the generation of new hydroxyl groups. This spectroscopic observation was directly corroborated by 2D-HSQC NMR analysis (Fig. 1). Specifically, the HSQC spectra revealed a pronounced disappearance of the peaks corresponding to the β-O-4 aryl ether linkages (specifically the Aα, Aβ, and Aγ signals) in the LML sample, providing definitive structural evidence for the laccase-mediated cleavage of these linkages, in strong agreement with the FTIR results. The increased vibration of the C-H bond at 2930 cm^{-1} in LML compared to the control sample suggests the side-chain cleavage

and demethoxylation, altering the functional groups of the resulting aromatic monomers [29]. In contrast, the characteristic aromatic bands at 1600–1500 cm^{-1} (C═C stretching) and 1510 cm^{-1} (aromatic C-H vibrations) displayed stable intensities. This confirmed the effective preservation of the benzene ring framework, a structural feature essential for the enhanced thermal stability and antioxidant properties of the modified lignin [30]. FTIR analysis confirmed that laccase-mediated modification successfully remodelled the molecular structure of lignin, selectively targeting the lignin side chains while preserving its aromatic core, in which the enriched hydroxyl content could enhance the reactivity of the modified lignin towards isocyanates.

To further elucidate the surface chemical changes induced by laccase modification, XPS analysis was performed on both unmodified and modified lignin (Fig. 1F). In the C1s spectra, the relative content of C-O decreased from 30.82% to 30.35% after modification, reflecting the oxidative cleavage of ether bonds during the laccase-catalysed radical process. More notably, in the O1s spectra, the proportion of C-OH/C-O-C oxygen increased significantly from 54.82% to 58.05%, accompanied by a decrease in C═O oxygen from 45.18% to 41.95%. These changes are consistent with β-O-4 cleavage events, which consume one ether linkage while simultaneously generating new hydroxyl groups. This finding is in excellent agreement with the ^{31}P NMR results, which quantitatively confirmed an increase in both phenolic hydroxyl (from 3.45 to 3.61 mmol/g) and aliphatic hydroxyl (from 1.21 to 1.52 mmol/g) contents after laccase treatment. The convergence of FTIR, ^{31}P NMR, and XPS evidence collectively supports the occurrence of partial β-O-4 bond cleavage during laccase modification, resulting in lignin with enhanced hydroxyl functionality and reduced molecular weight.

To evaluate the impact of enzymatic activity on lignin structural modification and hydroxyl enrichment, the secretion profile of *T. versicolor* was analysed (Fig. 1E). After a three-day cultivation of *T. versicolor*, laccase enzymatic activity reached 243.63 ± 8.78 U/L (CV = 3.60%), confirming the high reproducibility of this assay through multiple independent experiments. The laccase activity was approximately 198-fold higher than that of MnP and LiP, confirming its role as the primary driver of lignin modification. To overcome the steric limitations of direct enzymatic oxidation and extend laccase's oxidative capability toward recalcitrant non-phenolic structures, HBT was integrated into the optimised Day 3 supernatant system as a mediator [31]. In this laccase-mediator system, laccase first oxidises HBT to generate highly reactive radical intermediates. Then these intermediates diffuse into the sterically hindered lignin network and indirectly oxidise the otherwise non-phenolic substrates [32], thereby maximising the generation of reactive hydroxyl sites for subsequent polyurethane synthesis.

3.2. Interfacial architecture of lignin-based films

The efficacy of lignin activation on morphological homogeneity and interfacial compatibility is evident. The cross-sectional morphology of LPUs after cryo-fracturing was studied using SEM and significant differences in the cross-sectional morphologies of the films were observed (Fig. 2A). At 50k magnification, the control film (PU films) exhibited numerous internal voids with a pore diameter of 1585.92 nm because of the relatively loose native network structure of the polyurethane film. In contrast, LMLPF displayed a compact and smooth morphology with the pore diameter drastically reduced to 242.25 nm. This substantial structural densification further confirms that LML effectively acted as a crosslinking agent, integrating seamlessly into the PU matrix to form a continuous network that greatly minimises macroscopic defects.

The urethane formation was further evidenced in FTIR examination (Fig. 2B), which was performed to elucidate the molecular mechanism underlying the enhanced interfacial bonding. The successful synthesis of the lignin-polyurethane network was confirmed by the emergence of characteristic bands assigned to -NH groups (1536 cm^{-1}) [33] and -CN stretching (1258 cm^{-1}) [34], and the preservation of polyether soft segments (1090–1080 cm^{-1}) [35] alongside the complete disappearance of the -NCO groups at 2270 cm^{-1} [36]. Regarding lignin modification, the increased C-H stretching intensity (3000–2800 cm^{-1}) is consistent with the cleavage of β-O-4 linkages. The depolymerisation into lower molecular weight fragments reduced intermolecular aggregation, thereby enhancing the infrared absorption of aliphatic C-H groups (e.g., -OCH_3, -CH_2-, -CH-). This structural disruption, together with the increased hydroxyl groups, contributed to the improved solubility and homogeneity of the modified lignin. This improved compatibility facilitated a more efficient reaction with HDI, as corroborated by the notably higher intensity of the urethane-associated band at 1560 cm^{-1} in LMLPF compared to LPF. This spectroscopic evidence demonstrated that laccase modification, by enriching lignin with reactive aliphatic hydroxyls and flexible side chains, effectively disrupted the internal hydrogen-bond network and improved its compatibility. This facilitated a more efficient reaction with HDI, promoting the formation of a denser, structurally robust cross-linked network responsible for the enhanced rigidity and thermal stability of the LMLPF.

Swelling tests (Fig. 2C and Fig. 2D) were conducted to evaluate the network structure of the films. LMLPF-30% showed a lower swelling ratio (32.38 ± 6.78%) than LPF-30% (63.11 ± 2.23%, $p < 0.001$). Meanwhile, the crosslinking density of the LMLPFs is 39% higher than that of the LPFs (1.78×10^{-3} mol/cm^3). This enhancement was attributed to laccase modification, which activated lignin by increasing the accessibility and quantity of hydroxyl groups. These active sites facilitated a more complete reaction with isocyanates, promoting the formation of a denser urethane network [37]. Consistent with swelling theory, this highly cross-linked structure restricts solvent uptake, resulting in a more compact and rigid film.

In addition, Fig. 2E showed a notable decrease in crystallinity in LMLPFs compared to the LPFs, 32% of LMLPFs compared to 42% of LPFs at 30 wt% lignin content, which was attributed to the higher crosslink density within the LMLPF network. LML with more reactive hydroxyl sites served as a more effective macromolecular crosslinking agent that promoted better incorporation within the polymer network and increased crosslinking density [38]. Therefore, these additional crosslinks severely restricted the mobility of the polyurethane soft segments, inhibiting the chain ordering required for crystallisation, and created a more densely cross-linked, amorphous network. It should be emphasised that this defect-free interface and high crosslinking density were the direct prerequisite for the superior mechanical rigidity and thermal resistance observed in the LMLPFs.

Different letters (a-c) indicate statistically significant differences ($p < 0.05$, one-way ANOVA with Tukey's HSD post-hoc test).

3.3. Emergence of enhanced mechanical and thermal properties

The LMLPFs exhibited significantly superior mechanical performance, especially at 30% lignin content. The tensile strength and elastic modulus of the LMLPFs increased to 31.49 MPa and 215.23 MPa, respectively, with approximately 25% and 60% improvements over those of LPFs (Table 1). This enhancement was primarily attributed to the higher crosslinking density in LMLPFs. As aforementioned, confirmed by ^{3} ^{1}P NMR analysis, laccase modification bioconverts lignin as a more effective multifunctional crosslinker by increasing the hydroxyl group contents and thereby forming a denser covalent network. Besides, the 60% increase in elastic modulus also confirms this. Moreover, though the elongation at break decreased for both groups, attributed to the increased network rigidity and crosslinking within the mixtures, the modified LMLPF retained superior flexibility compared to LPF. This improvement was ascribed to the introduction of flexible aliphatic chains into lignin during modification, which served as soft spacers to alleviate the stiffness of the aromatic core. Additionally, the improved dispersion of LML prevents the formation of brittle phases and stress concentrators and endows the film with higher extensibility. Importantly, LMLPF-30% also showed significantly higher mechanical performance compared to LPF-30% (tensile strength: $p = 0.023$; elastic

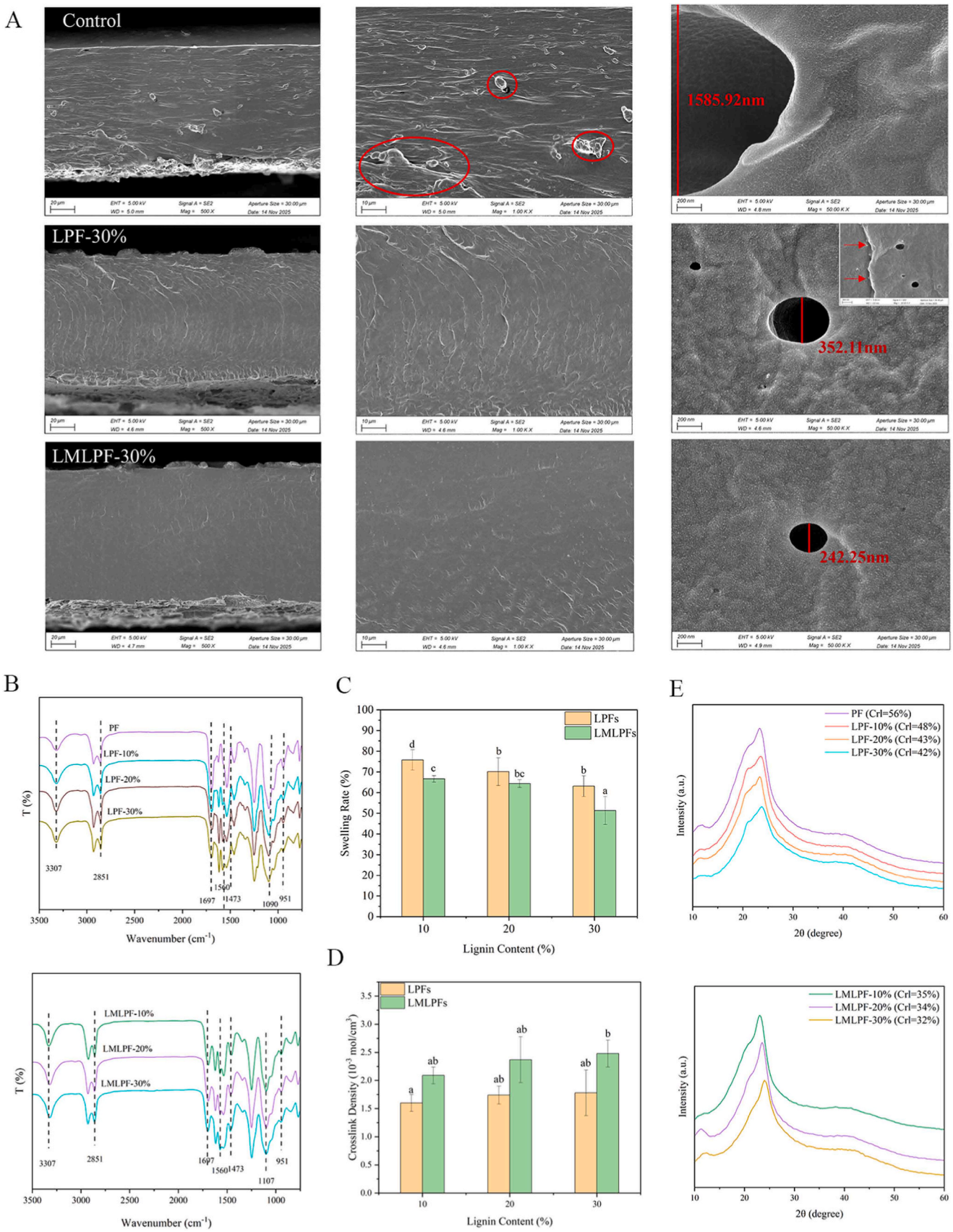

Fig. 2. Effect of lignin activation on lignin-based films interfacial compatibility: A. SEM fracture surfaces of PU films after cryo-fractured, B. FTIR spectra of LPFs (top) and LMLPFs (bottom), C. swelling rate properties of lignin-based films, D. crosslink density of lignin-based films, E. XRD patterns of LPFs (top) and LMLPFs (bottom).

modulus: $p < 0.001$), confirming the effectiveness of the lignin modification strategy.

The thermal stability of the PU films was evaluated by TGA, revealing a two-stage thermal decomposition process for all samples (Fig. 3). The initial stage (200–375 ℃) corresponded to the degradation of urethane linkages and lignin side-chains [39] like ether bonds cleavage, dehydration and decarboxylation, as well as the elimination of carbon dioxide and water [40]. The second stage of thermal decomposition occurred between 375 and 500 °C, attributed to the decomposition of the more stable aromatic structures [41,42]. Notably, increasing the lignin content elevated the onset decomposition temperature ($T_{5\%}$), with this enhancement being significantly more pronounced in LMLPFs (273 ℃ to 280 ℃) compared to LPFs (273 ℃ to 277 ℃). This superior stability was directly attributed to the laccase-mediated optimisation of lignin: the enriched reactive hydroxyl groups and reduced steric hindrance facilitated the efficient covalent incorporation of LML into the polyurethane matrix. Functioning as rigid aromatic crosslinking centres, LML promoted the formation of a denser three-dimensional network that restricted chain mobility and increased the activation energy for degradation, thereby effectively inhibiting bond cleavage and enhancing the overall thermal resistance of the material.

As presented in Fig. 3A, increasing the lignin content from 10% to 30%, the T_g of the LMLPFs rose from −13.58 ℃ to 9.30 ℃. Lignin can serve not only as a cross-linking agent but also as a hard segment in the formation of three-dimensional network polyurethane polymers [41]. Meanwhile, lignin is an amorphous, rigid macromolecule possessing a high T_g [43]. Its incorporation with the polyurethane enhances cross-link density and introduces strong intermolecular forces like hydrogen bonds that effectively restrict soft segment mobility [44]. This enhancement was attributed to the enriched reactive hydroxyl groups in LML, which fostered a denser covalent network that restricts chain motion more effectively than the weaker physical interactions in LPFs. The change in heat capacity (ΔCp) increased from 0.30 to 0.38 J/(g·K). This trend might result from two factors. As evidenced by the XRD results, LMLPF exhibited lower crystallinity compared to LPF, the expansion of the amorphous fraction resulted in an increase in the heat capacity (ΔCp) [45]. Also, laccase modification enriched LML with phenolic and aliphatic hydroxyl groups that formed extensive hydrogen-bonding networks in the amorphous phase. Study has shown that the addition of hydroxyl groups greatly strengthens the hydrogen bond network and increases the macroscopic specific heat capacity [46]. Breaking these hydrogen bonds requires extra thermal energy, which also raises the ΔCp.

The DMA results (Fig. 3B) provide direct evidence for the role of modified lignin as an active crosslinker in the polyurethane network. The neat PU film exhibited a remarkably low storage modulus (124.19 MPa at −29 ℃) and lacked a well-defined tan δ peak, indicating an insufficiently crosslinked network. Upon incorporation of unmodified lignin, the storage modulus increased by approximately one order of magnitude to 1200 MPa, suggesting that pristine lignin can function as a crosslink through the reaction of its hydroxyl groups with isocyanate.

Table 2
Mechanical properties of the LPFs and LMLPFs.

Sample name	Tensile strength /MPa	Elasticity modulus /MPa	Elongation at break /%
PF	11.39 ± 3.07	57.81 ± 3.96	334.07 ± 109.11
LPF-10%	12.89 ± 1.29	58.88 ± 9.33	288.34 ± 94.86
LPF-20%	15.31 ± 1.53	82.73 ± 8.60	236.07 ± 59.71
LPF-30%	25.21 ± 3.55	134.40 ± 16.26	228.20 ± 25.19
LMLPF-10%	16.07 ± 2.74	78.34 ± 10.64	252.13 ± 14.09
LMLPF-20%	18.24 ± 2.19	102.63 ± 11.54	216.23 ± 17.80
LMLPF-30%	31.49 ± 4.18	215.23 ± 7.64	177.93 ± 27.59

However, the relatively low T_g and broad tan δ peak suggest limited crosslinking efficiency, likely attributable to the high molecular weight and poor hydroxyl accessibility of unmodified lignin. In contrast, the modified lignin-based PU film exhibited a further increase in storage modulus to approximately 2000 MPa, accompanied by a higher T_g and a sharper tan δ peak, indicating enhanced crosslinking density. This improvement can be attributed to the synergistic effects of molecular weight reduction and the introduction of additional accessible aliphatic hydroxyl groups. Collectively, these results demonstrated that chemical modification effectively transformed lignin from a passive filler into an active crosslinker that substantially reinforces the polyurethane network.

The enhanced thermal stability of the polyurethane films upon laccase modification, as confirmed by both TGA and DSC analyses, can be attributed to crucial structural alterations at the molecular level. Specifically, the enrichment of active functional groups in the LML facilitated the formation of a more densely crosslinked and structurally robust three-dimensional network. Crucially, this significantly improved interfacial compatibility, eliminating the interfacial voids and defects that typically act as weak points for thermal degradation. The covalent incorporation of LML into the polyurethane network not only restricts soft segment mobility, thereby elevating the glass transition temperature, but also enhances the overall crosslinking density, resulting in significant network reinforcement. Supported by this reinforced architecture, the LML-based films exhibited performance superior to recent literature benchmarks. At 30 wt% lignin content, it achieves a tensile strength of 31.49 MPa, which is approximately 2–3 times higher than those of counterparts reported in previous studies, such as 13.20 MPa (at 37.4 wt% lignin content) [14] and 10.60 MPa (at 30 wt% lignin content) [47]. Notably, this high strength does not compromise ductility; our sample maintains a high elongation at break (177.93%), outperforming 142.77% [48]. Additionally, the elevated thermal stability ($T_{10\%}$ of 298.00 ℃) further evidences the formation of a robust cross-linked network.

3.4. Existing studies on lignin modification and lignin-based polyurethane systems

To further contextualise the advances achieved in this study, a comprehensive comparison with representative lignin modification strategies reported in the literature is summarised in Table 3. Compared with chemical modification approaches and previous enzymatic methods, the crude laccase/HBT-mediated modification developed in this work achieves simultaneous enhancement of both aliphatic and phenolic hydroxyl content under mild aqueous conditions, resulting in PU films with superior comprehensive performance. This strategy offers a low-cost, energy-efficient, and environmentally friendly route for preparing high-performance lignin-based PU films.

4. Conclusions

This study presents a green evolutionary enzymatic strategy using a *T. versicolor* laccase system with HBT to functionalize AL into a more reactive LML for the preparation of lignin-based films. The core innovation centred on the targeted laccase-mediated modification, which effectively cleaved ether bonds and induced demethoxylation. This mild enzymatic modification increased both phenolic hydroxyl (from 3.45 to 3.61 mmol/g) and aliphatic hydroxyl (from 1.21 to 1.52 mmol/g) contents while preserving the essential aromatic structure. As a result, LML exhibited improved reactivity compared to unmodified AL, enabling its enhanced participation in crosslinking reactions. At 30% lignin content, LMLPFs demonstrated a denser and more homogeneous network, exhibiting a higher crosslink density (2.48×10^{-3} mol/cm^3) compared to LPFs (1.78×10^{-3} mol/cm^3). This structural improvement contributed to enhanced mechanical properties, with tensile strength and elastic modulus reaching 31.49 MPa and 215.23 MPa (increases of

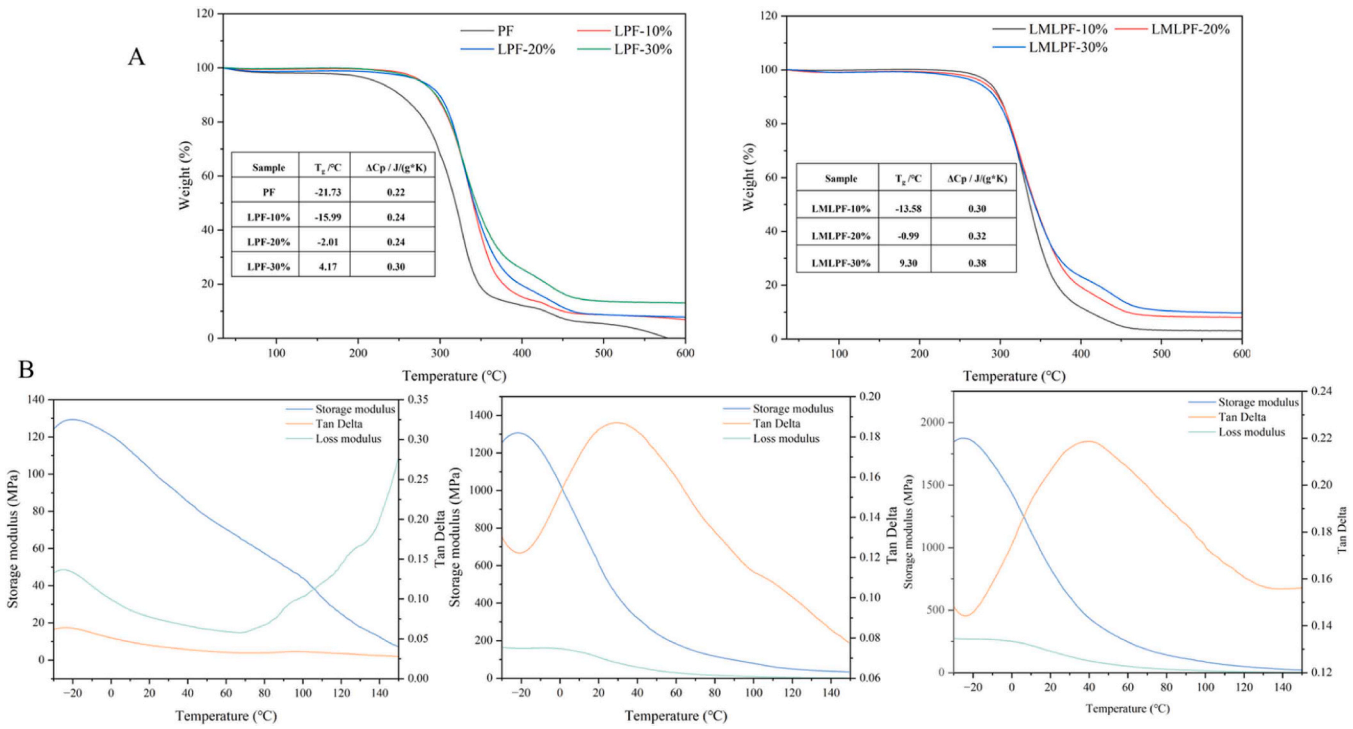

Fig. 3. Thermal properties of lignin-based films: A. thermal stability of LPFs (left) and LMLPFs (right), B. dynamic mechanical properties of PU (left), LPF (middle) and LMLPF (right).

Table 3
Comparison of representative prior studies on laccase-modified lignin and lignin-based polyurethane (PU) systems with the present work.

Lignin modification approach	Modifying agent & reaction conditions.	Lignin structural changes	Performance	Energy, cost & environmental considerations
Co-solvent enhanced lignocellulosic fractionation pretreatment [14].	THF and H_2SO_4; harsh (150, 160 and 180 ℃).	Aliphatic hydroxyl content decreased, and phenolic hydroxyl content increased.	Tensile strength (13.20 MPa) and elongation at break (24.23%).	High energy consumption, moderate cost and volatile organic solvent usage.
Two-step esterification modification [15].	DMF, DMAP and DCC; harsh (80 ℃ for 48 h).	Lignin carboxyl content increased.	Tensile strength (10.00 MPa) and elongation at break (34.00%).	High cost of chemical reagents, moderate energy consumption and environmentally friendly.
HDI modification [16].	HDI and THF; prolonged (50 ℃ for 6 h under nitrogen atmosphere).	$T_{5\%}$ decreased.	Tensile strength (12.07 MPa).	Low energy consumption, moderate cost and volatile organic solvent usage.
Modified by laccase enzyme in the presence of TEMPO [18].	Commercially purified laccase and TEMPO; prolonged (24 h at room temperature).	Decrease in particle size.	Wet shear strength (1.429 MPa) and viscosity (7.92 Pa·s).	High energy consumption, moderate cost.
Enzymatic modification [19].	Purified laccase from *Trametes trogii*; prolonged (pH 6.5 for 24 h).	An increase in aliphatic hydroxyl groups and the content of phenolic hydroxyl groups decreased slightly.	The purified laccase showed thermal stability, phenolic hydroxyl and methoxy groups decreased.	Moderate energy consumption, moderate cost.
Corn straw enzymatic hydrolysed lignin [49].	Commercial corn straw enzymatic hydrolysed lignin.	The phenolic hydroxyl content of the lignin was 3.64%.	Shear strength under room temperature (19.1 MPa).	Low energy consumption, low to moderate cost and environmentally friendly.
Modified by laccase enzyme and HBT (this work).	Crude *T. versicolor* broth and HBT (40 ℃ for 6 h).	Aliphatic and phenolic hydroxyl content increased.	Tensile strength (31.49 MPa), elastic modulus (215.23 MPa), elongation at break (177.93%) and thermal stability ($T_{5\%}$ = 280 ℃).	Low energy consumption, the lowest among enzymatic approaches and environmentally friendly.

approximately 25% and 60%, respectively), along with improved thermal stability ($T_{5\%}$ = 280 ℃). These findings suggest that laccase-mediated modification is a viable and environmentally friendly approach for the high-value utilisation of lignin, offering a potential pathway toward the development of lignin-based biocomposites with improved structural performance.

CRediT authorship contribution statement

Jingjing Liao: Writing – review & editing. **Yonghui Zhou:** Writing – review & editing. **Mizi Fan:** Methodology. **Xiaojian Zhou:** Methodology. **Yan Xia:** Supervision, Funding acquisition. **Yingjie Wang:** Formal analysis. **Jieyu Yang:** Writing – original draft, Conceptualization. **Guanben Du:** Conceptualization. **Yu Qin:** Formal analysis.

Declaration of competing interest

The authors declare that they have no known competing financial interests or personal relationships that could have appeared to influence the work reported in this paper.

Acknowledgements

The authors are grateful for the financial support from the Regional Project of the National Natural Science Foundation of China (32260362), the Joint Project of Yunnan Agricultural Basic Research (202401BD070001–025), the Foreign Experts Project of Yunnan Province (202505AO120007), the Reserve Talent Project for Young and Middle-aged Academic and Technical Leaders of Yunnan Province (202405AC350033), the European Union, EIC Pathfinder 2023 (HORIZON-EIC-2023-PATHFINDEROPEN-01) (No. 101130895) and the 111 Project (D21027).

Data availability

Data will be made available on request.

References

[1] Y. Su, S. Zhang, Y. Xiong, H. Zhang, Detecting the inner mechanism of agglomeration behaviors and product properties during fast pyrolysis of lignin via alkaline additives, Fuel Process. Technol. 238 (2022) 107528, https://doi.org/10.1016/j.fuproc.2022.107528.
[2] S. Kim, H. Chung, Convenient Cross-Linking Control of Lignin-Based Polymers Influencing Structure–Property Relationships, ACS Sustain. Chem. Eng. 11 (2023) 1709–1719, https://doi.org/10.1021/acssuschemeng.2c05651.
[3] S.K. Shin, Y.J. Ko, J.E. Hyeon, S.O. Han, Studies of advanced lignin valorization based on various types of lignolytic enzymes and microbes, Bioresour. Technol. 289 (2019) 121728, https://doi.org/10.1016/j.biortech.2019.121728.
[4] B.M. Upton, A.M. Kasko, Strategies for the Conversion of Lignin to High-Value Polymeric Materials: Review and Perspective, Chem. Rev. 116 (2016) 2275–2306, https://doi.org/10.1021/acs.chemrev.5b00345.
[5] M. Xue, S. Hu, S. Zhang, J. Ou, H. Chen, Y. Liao, F. Yue, Flexible and Heat-Resisting Lignin-Based Epoxy Resins by Hardwood Kraft Low-Molecular-Weight Lignin as a Sustainable Substitute for Bisphenol A, ACS Sustain. Chem. Eng. 11 (2023) 16774–16784, https://doi.org/10.1021/acssuschemeng.3c04898.
[6] J. Hu, Z. Xin, Y. Huang, C. Geng, H. Jia, J. Xu, X. Wang, Rational design of molecularly modified lignin-based degradable nanocomposite fibers and their synergistic application of anti-microbial, UV-shielding, radioactive iodine trapping function based on green chemistry orientation, Chem. Eng. J. 524 (2025) 169240, https://doi.org/10.1016/j.cej.2025.169240.
[7] F. Tan, F. Lu, J. Wei, X. Wang, J. Zhou, J. Xu, Synergistic enhancement of electrochemical performance in lignin-based carbon aerogel supercapacitors through phytic acid-induced spherical structure formation and dual P/S heteroatom doping, J. Bioresour. Bioprod. (2026) 100234, https://doi.org/10.1016/j.jobab.2026.100234.
[8] F. Tan, F. Lu, Y. Yan, Y. Wang, X. Wang, J. Zhou, J. Xu, Progress in preparation strategies for lignin-derived carbon aerogels and the regulation of their supercapacitor performance, Fuel 407 (2026) 137371, https://doi.org/10.1016/j.fuel.2025.137371.
[9] G. Griffini, V. Passoni, R. Suriano, M. Levi, S. Turri, Polyurethane Coatings Based on Chemically Unmodified Fractionated Lignin, ACS Sustain. Chem. Eng. 3 (2015) 1145–1154, https://doi.org/10.1021/acssuschemeng.5b00073.
[10] A.T. Smit, E. Bellinetto, T. Dezaire, O. Boumezgane, L.A. Riddell, S. Turri, M. Hoek, P.C.A. Bruijnincx, G. Griffini, Tuning the Properties of Biobased PU Coatings via Selective Lignin Fractionation and Partial Depolymerization, ACS Sustain. Chem. Eng. 11 (2023) 7193–7202, https://doi.org/10.1021/acssuschemeng.3c00889.
[11] F.R. Vieira, S. Magina, D.V. Evtuguin, A. Barros-Timmons, Lignin as a Renewable Building Block for Sustainable Polyurethanes, Materials 15 (2022) 6182, https://doi.org/10.3390/ma15176182.
[12] L.D. Antonino, I. Sumerskii, A. Potthast, T. Rosenau, M.I. Felisberti, D.J. dos Santos, Lignin-Based Polyurethanes from the Blocked Isocyanate Approach: Synthesis and Characterization, ACS Omega 8 (2023) 27621–27633, https://doi.org/10.1021/acsomega.3c03422.
[13] C. Weng, X. Peng, Y. Han, Depolymerization and conversion of lignin to value-added bioproducts by microbial and enzymatic catalysis, Biotechnol. Biofuels 14 (2021) 84, https://doi.org/10.1186/s13068-021-01934-w.
[14] Y.-Y. Wang, P. Sengupta, B. Scheidemantle, Y. Pu, C.E. Wyman, C.M. Cai, A. J. Ragauskas, Effects of CELF Pretreatment Severity on Lignin Structure and the Lignin-Based Polyurethane Properties, Front. Energy Res. 8 (2020), https://doi.org/10.3389/fenrg.2020.00149.
[15] Q. Xie, J. Zhou, H. Sun, J. Fu, M. Cui, X. Wang, F. Li, J. Zhu, J. Chen, Castor oil graphted lignin-based polyurethane film with excellent barrier properties, Prog. Org. Coat. 211 (2026) 109767, https://doi.org/10.1016/j.porgcoat.2025.109767.
[16] T. Wu, X. Li, X. Ma, J. Ye, L. Shen, W. Tan, Modification of lignin by hexamethylene diisocyanate to synthesize lignin-based polyurethane as an organic polymer for marine polyurethane anticorrosive coatings, Mater. Res. Express 9 (2022) 105302, https://doi.org/10.1088/2053-1591/ac95fc.
[17] M.B. Agustin, D.M. de Carvalho, M.H. Lahtinen, K. Hilden, T. Lundell, K. S. Mikkonen, Laccase as a Tool in Building Advanced Lignin-Based Materials, ChemSusChem 14 (2021) 4615–4635, https://doi.org/10.1002/cssc.202101169.
[18] S. Pradyawong, G. Qi, X.S. Sun, D. Wang, Laccase/TEMPO-modified lignin improved soy-protein-based adhesives: adhesion performance and properties, Int. J. Adhes. Adhes. 91 (2019) 116–122, https://doi.org/10.1016/j.ijadhadh.2019.03.005.
[19] M.-Q. Ai, F.-F. Wang, F. Huang, Purification and characterization of a thermostable laccase from trametes trogii and its ability in modification of kraft lignin 25 (2015) 1361–1370, https://doi.org/10.4014/jmb.1502.02022.
[20] S. Zhang, Z. Dong, J. Shi, C. Yang, Y. Fang, G. Chen, H. Chen, C. Tian, Enzymatic hydrolysis of corn stover lignin by laccase, lignin peroxidase, and manganese peroxidase, Bioresour. Technol. 361 (2022) 127699, https://doi.org/10.1016/j.biortech.2022.127699.
[21] J. Li, P. Wang, N. Salam, X. Li, M. Ahmad, Y. Tian, L. Duan, L. Huang, M. Xiao, X. Mou, W. Li, Unraveling bacteria-mediated degradation of lignin-derived aromatic compounds in a freshwater environment, Sci. Total Environ. 749 (2020) 141236, https://doi.org/10.1016/j.scitotenv.2020.141236.
[22] T. Arnstadt, B. Hoppe, T. Kahl, H. Kellner, D. Krüger, C. Bässler, J. Bauhus, M. Hofrichter, Patterns of laccase and peroxidases in coarse woody debris of Fagus sylvatica, Picea abies and Pinus sylvestris and their relation to different wood parameters, Eur. J. For. Res. 135 (2016) 109–124, https://doi.org/10.1007/s10342-015-0920-0.
[23] M. Wadekar, W. Eevers, R. Vendamme, Influencing the properties of LigninPU films by changing copolyol chain length, lignin content and NCO/OH mol ratio, Ind. Crops Prod. 141 (2019) 111655, https://doi.org/10.1016/j.indcrop.2019.111655.
[24] H. Yoshida, R. Mörck, K.P. Kringstad, H. Hatakeyama, Kraft lignin in polyurethanes I. Mechanical properties of polyurethanes from a kraft lignin–polyether triol–polymeric MDI system, J. Appl. Polym. Sci. 34 (1987) 1187–1198, https://doi.org/10.1002/app.1987.070340326.
[25] Z. Jia, C. Lu, P. Zhou, L. Wang, Preparation and characterization of high boiling solvent lignin-based polyurethane film with lignin as the only hydroxyl group provider, RSC Adv. 5 (2015) 53949–53955, https://doi.org/10.1039/C5RA09477A.
[26] S. Zhang, Z. Dong, J. Shi, C. Yang, Y. Fang, G. Chen, H. Chen, C. Tian, Enzymatic hydrolysis of corn stover lignin by laccase, lignin peroxidase, and manganese peroxidase, Bioresour. Technol. 361 (2022) 127699, https://doi.org/10.1016/j.biortech.2022.127699.
[27] Y. Song, Z. Wang, N. Yan, R. Zhang, J. Li, Demethylation of Wheat Straw Alkali Lignin for Application in Phenol Formaldehyde Adhesives, Polymers 8 (2016) 209, https://doi.org/10.3390/polym8060209.
[28] S.K. Singh, P.L. Dhepe, Isolation of lignin by organosolv process from different varieties of rice husk: Understanding their physical and chemical properties, Bioresour. Technol. 221 (2016) 310–317, https://doi.org/10.1016/j.biortech.2016.09.042.
[29] H. Yang, R. Yan, H. Chen, D.H. Lee, C. Zheng, Characteristics of hemicellulose, cellulose and lignin pyrolysis, Fuel 86 (2007) 1781–1788, https://doi.org/10.1016/j.fuel.2006.12.013.
[30] A. Rahmani, A. Abdulkhani, A. Ashori, J. Hosseinzadeh, Development of high-performance biocomposites through lignin modification and fiber reinforcement, Sci. Rep. 14 (2024) 28932, https://doi.org/10.1038/s41598-024-80256-x.
[31] R. Hilgers, J.-P. Vincken, H. Gruppen, M.A. Kabel, Laccase/Mediator Systems: Their Reactivity toward Phenolic Lignin Structures, ACS Sustain. Chem. Eng. 6 (2018) 2037–2046, https://doi.org/10.1021/acssuschemeng.7b03451.
[32] G. Janusz, E. Skwarek, A. Pawlik, Potential of Laccase as a Tool for Biodegradation of Wastewater Micropollutants, Water 15 (2023) 3770, https://doi.org/10.3390/w15213770.
[33] S.Elisabeth Klein, J. Rumpf, P. Kusch, R. Albach, M. Rehahn, S. Witzleben, M. Schulze, Unmodified kraft lignin isolated at room temperature from aqueous solution for preparation of highly flexible transparent polyurethane coatings, RSC Adv. 8 (2018) 40765–40777, https://doi.org/10.1039/C8RA08579J.
[34] J. Li, B. Wang, K. Chen, X. Tian, J. Zeng, J. Xu, W. Gao, The use of lignin as cross-linker for polyurethane foam for potential application in adsorbing materials, BioResources 12 (2017) 8653–8671, https://doi.org/10.15376/biores.12.4.8653-8671.
[35] S.M. Manap, A. Ahmad, F.H. Anuar, Characterization of poly(L-lactide/Propylene glycol) based polyurethane films using ATR-FTIR spectroscopy, AIP Conf. Proc. 1784 (2016), https://doi.org/10.1063/1.4966758.
[36] L.I.U. Ruowang, C. Yuye, Z. Chuyin, P. a N. Weijing, Study on the Solvent-free Synthesis and Properties of Waterborne Polyurethane, Leather Sci. Eng. 33 (2023) 54–59, https://doi.org/10.19677/j.issn.1004-7964.2023.01.009.
[37] B.-S. Chiou, P.E. Schoen, Effects of crosslinking on thermal and mechanical properties of polyurethanes, J. Appl. Polym. Sci. 83 (2002) 212–223, https://doi.org/10.1002/app.10056.
[38] H. Zhou, X. Qiu, D. Yang, S. Xie, Laccase and Xylanase Incubation Enhanced the Sulfomethylation Reactivity of Alkali Lignin, ACS Sustain. Chem. Eng. 4 (2016) 1248–1254, https://doi.org/10.1021/acssuschemeng.5b01291.
[39] H. Wang, Y. Ni, M.S. Jahan, Z. Liu, T. Schafer, Stability of cross-linked acetic acid lignin-containing polyurethane, J. Therm. Anal. Calor. 103 (2010) 293–302, https://doi.org/10.1007/s10973-010-1052-x.

[40] T.Ç. Çanak, K. Kaya, I.E. Serhatlı, Boron containing UV-curable epoxy acrylate coatings, Prog. Org. Coat. 77 (2014) 1911–1918, https://doi.org/10.1016/j.porgcoat.2014.06.021.
[41] J.C. Domínguez, M. Oliet, M.V. Alonso, M.A. Gilarranz, F. Rodríguez, Thermal stability and pyrolysis kinetics of organosolv lignins obtained from *Eucalyptus globulus*, Ind. Crops Prod. 27 (2008) 150–156, https://doi.org/10.1016/j.indcrop.2007.07.006.
[42] Y. Kurimoto, M. Takeda, S. Doi, Y. Tamura, H. Ono, Network structures and thermal properties of polyurethane films prepared from liquefied wood, Bioresour. Technol. 77 (2001) 33–40, https://doi.org/10.1016/S0960-8524(00)00136-X.
[43] R.V. Gadhave, P.A. Mahanwar, P.T. Gadekar, Lignin-Polyurethane Based Biodegradable Foam, Open J. Polym. Chem. 08 (2018) 1, https://doi.org/10.4236/OJPCHEM.2018.81001.
[44] J.R. Gouveia, C.L. da Costa, L.B. Tavares, D.J. dos Santos, Synthesis of Lignin-Based Polyurethanes: A Mini-Review, Mini-Rev. Org. Chem. 16 (2019) 345–352, https://doi.org/10.2174/1570193X15666180514125817.
[45] K.-H. Illers, The heat capacity of poly(oxymethylene) as a function of crystailinity, Polym. Bull. 15 (1986) 265–270, https://doi.org/10.1007/BF00255073.
[46] R. Fareghi-Alamdari, R. Hatefipour, M. Rakhshi, N. Zekri, Novel diol functionalized dicationic ionic liquids: synthesis, characterization and DFT calculations on H-bonding influence on thermophysical properties, RSC Adv. 6 (2016) 78636–78647, https://doi.org/10.1039/C6RA17188E.
[47] A. Cassales, L.A. Ramos, E. Frollini, Synthesis of bio-based polyurethanes from Kraft lignin and castor oil with simultaneous film formation, Int. J. Biol. Macromol. 145 (2020) 28–41, https://doi.org/10.1016/j.ijbiomac.2019.12.173.
[48] X. Chen, Z. Li, L. Zhang, H. Wang, C. Qiu, X. Fan, S. Sun, Preparation of a novel lignin-based film with high solid content and its physicochemical characteristics, Ind. Crops Prod. 164 (2021) 113396, https://doi.org/10.1016/j.indcrop.2021.113396.
[49] N. Sun, Y. Lai, Y. Xu, L. Wang, X. Shang, M. Di, X. Kong, Preparations and properties of polyurethane adhesives modified by corn straw lignin, BioResources 15 (2020) 3970–3983, https://doi.org/10.15376/biores.15.2.3970-3983.